Duc Nguyen*, Stefan Miska*, Mengjiao Yu*, Robert Mitchell*

TEMPERATURE PROFILES IN DIRECTIONAL AND HORIZONTAL WELLS – THE EFFECT OF DRAG FORCES

INTRODUCTION

Deep and highly deviated wells have become more and more common due to their ability to reach for deeper and further reserves and the considerable benefits that they have. However, unusual temperature and pressure behavior in such wells are likely to cause intricate wellbore stability problems, which could lead to more expensive drilling operations.

Drilling fluid circulation plays an important role in cooling the well and transporting cuttings. During drilling oil and gas wells, cuttings are carried by the drilling fluid in the annulus and out of the borehole. Because of mechanical and hydraulic friction this process generates heat, which is then transferred by advection along the borehole and exchanged with the formation by conduction. As a result, the surrounding rocks are heated up and cause higher stresses and change in pore pressure around the borehole, leading to wellbore instability.

Since oil-based drilling fluids offer low formation damage and high wellbore stability, they are more frequently used as a method of controlling shale instability. However, oil-based fluids have relatively low heat capacity, thus they are sensitive to the generated heat, and sometimes this can result in significant downhole overheating of drilling fluids. Consequently, stresses and pore pressures vary around the borehole, causing wellbore instability and operational problems such as stuck casing and drillpipe.

The purpose of this study is to investigate the physical phenomena associated with the overheating of drilling fluids and their effects on wellbore stability. The outcomes of the research are mechanistic and computer models that could be utilized to predict the temperature profiles of drilling fluids in drillpipe, annulus and formation. Moreover, they could also

* The University of Tulsa, USA

be combined with other models to produce a more comprehensive model, or used in other studies in which wellbore temperature profiles are required.

Semi-analytical temperature model

An analytical temperature model for vertical wells based on existing literature is investigated. Then, it is expanded to have a wider application with less simplification. The resulting model is capable of predicting temperature profiles for directional wells with the consideration of mechanical friction.

1. VERTICAL WELL WITH NO HEAT SOURCE

This analytical model to predict temperature profiles of drilling fluid in a vertical well is explained in detail by Karstad [2], and by Hasan and Kabir [7]. For reviewing purpose, it is summarized as follows:

Basic assumptions:

- Incompressible fluid with constant properties.
- No radiation heat transfer.
- Formation properties are independent of temperature.
- No heat transfer in pore space fluids in the formation.
- Radial temperature gradient of fluid is negligible.
- No source or sink of heat.

A control volume with heat rates into and out of the well element for a forward circulation is shown in Appendix C – Figure 2. Heat transfer is assumed to be steady state within the wellbore, and transient between the formation and wellbore.

Heat rate in drillpipe at z: $q_d(z) = \dot{m} c_{p,fl} T_d(z)$ (1)

Heat rate in annulus at z: $q_a(z) = \dot{m} c_{p,fl} T_a(z)$ (2)

Heat rate from annulus to drill pipe: $q_{ad} = \frac{\dot{m} c_{p,fl}}{B}(T_a - T_d)dz$ (3)

where: $B = \frac{\dot{m} c_{p,fl}}{2\pi r_d U_d}$ (4)

Heat rate from formation to annulus: $q_f = 2\pi r_w U_a (T_w - T_a) dz$ (5)

The transient heat flow from the formation to the wellbore wall is expressed as:

$$q_f = \frac{2\pi k_f}{f(t_D)}(T_{fi} - T_w)dz \quad (6)$$

where:

$f(t_D)$ – dimensionless time function and dependson the formation – borehole boundary conditions. Different $f(t_D)$ models are aummarized in Appendix A,

T_{fi} – initial formation temperature and is approximated as:

$$T_{fi} = T_{sf} + G_t z \tag{7}$$

From equations (5) and (6), T_w can be eliminated to give:

$$q_f = \frac{\dot{m} c_{p,fl}}{A}(T_{fi} - T_a)dz \tag{8}$$

where: $$A = \frac{\dot{m} c_{p,fl}}{2\pi r_w U_a}\left[1 + \frac{r_w U_a f(t_D)}{k_f}\right] \tag{9}$$

Energy balance is then applied to the control volume:

– In drillpipe: $q_d(z) + q_{ad} = q_d(z + dz)$ (10)

– In annulus: $q_a(z + dz) + q_f = q_a(z) + q_{ad}$ (11)

Combining equations (1), (2), (3), (8), (10) and (11) yields:

$$AB\frac{d^2 T_d}{dz^2} - B\frac{dT_d}{dz} - T_d + T_{sf} + G_t z = 0 \tag{12}$$

General solution to equation (12) for temperature in drillpipe:

$$T_d = \eta e^{\lambda_1 z} + \xi e^{\lambda_2 z} + G_t z - BG_t + T_{sf} \tag{13}$$

where:

$$\lambda_1 = \frac{1}{2A}\left(1 - \sqrt{1 + \frac{4A}{B}}\right)$$
$$\lambda_2 = \frac{1}{2A}\left(1 + \sqrt{1 + \frac{4A}{B}}\right) \tag{14}$$

η and ξ are obtained from the following boundary conditions:

– At wellhead, the temperature going into the drillpipe is the controlled inlet fluid temperature:

$$T_d(z = 0) = T_{inlet} \tag{15}$$

– At bottomhole, the heat exchange between drillpipe and annular fluid is zero:

$$\left.\frac{dT_d}{dz}\right|_{z=MD} = 0 \tag{16}$$

Result:

$$\begin{aligned}\eta &= -\frac{(T_{inlet} + BG_t - T_{sf})\lambda_2 e^{\lambda_2 MD} + G_t}{\lambda_1 e^{\lambda_1 MD} - \lambda_2 e^{\lambda_2 MD}} \\ \xi &= \frac{(T_{inlet} + BG_t - T_{sf})\lambda_1 e^{\lambda_1 MD} + G_t}{\lambda_1 e^{\lambda_1 MD} - \lambda_2 e^{\lambda_2 MD}}\end{aligned} \tag{17}$$

Finally, the annular fluid temperature and wellbore wall temperature can be obtained:

$$T_a = (1+\lambda_1 B)\eta e^{\lambda_1 z} + (1+\lambda_2 B)\xi e^{\lambda_2 z} + G_t z + T_{sf} \tag{18}$$

$$T_w = B\frac{dT_d}{dz} + T_d = T_a + (T_{sf} + G_t z - T_a)\frac{\dot{m}c_{p,f}}{2\pi r_w U_a A} \tag{19}$$

A similar analysis can be conducted to obtain the temperature profile for drilling fluid in reverse circulation condition. The direction of heat rates and boundary conditions are modified accordingly.

2. DIRECTIONAL WELL WITH HEAT SOURCE

The above temperature model is useful for obtaining temperature profile in a vertical well only. So, in order to cope with deviated wellbores, the model needs adjustment. Assume that the well path can be obtained from a survey. It is then discretized into n small parts so that the whole path is comprised of n straight sections. This is achieved by performing interpolation between 2 survey stations using minimum curvature method (more details can be found in the work of Sawaryn and Thorogood [9]).

Applying the above analysis for section i, and taking into account the existence of the heat source, q_s, the energy balance for the annulus – equation (11) – is modified as:

$$q_a(z+dz) + q_f + q_s = q_a(z) + q_{ad} \tag{20}$$

Assume a constant heat rate $\dot{q}_{friction}$ is generated in the whole wellbore within a time interval. For simplification, this heat source is considered evenly distributed along the measured depth:

$$q_s = \frac{\dot{q}_{friction}}{MD_{total}}dz \tag{21}$$

Performing a similar procedure that led to equations (13) and (18), one obtains:

$$T_{d,i} = \eta_i e^{\lambda_1 z} + \xi_i e^{\lambda_2 z} + G_t z Cos\theta_i - BG_t Cos\theta_i + T_{sf,i} + \frac{\dot{q}_{friction} A}{MD_{total} \dot{m} c_{p,fl}} \tag{22}$$

$$T_{a,i} = (1+\lambda_1 B)\eta_i e^{\lambda_1 z} + (1+\lambda_2 B)\xi_i e^{\lambda_2 z} + G_t z Cos\theta_i + T_{sf,i} + \frac{\dot{q}_{friction} A}{MD_{total} \dot{m} c_{p,fl}} \tag{23}$$

where:

L_i – length of section i
Q_i = inclinatio n angle of section i
$T_{sf,i}$ = $T_{sf} + G_t TVD_i$
TVD_i = true vertical depth of section i
η_i and ξ_i are unknowns and are determined from the modified boundary conditions:

$$\begin{aligned} &T_{d,1}(0) = T_{inlet} \\ &T_{d,i}(L_i) = T_{d,i+1}(0) \\ &T_{a,i}(L_i) = T_{a,i+1}(0) \\ &\left.\frac{dT_{d,n}}{dz}\right|_{z=L_n} = 0 \end{aligned} \tag{24}$$

Combining equations (22), (23) and (24) yields the following equation system:

$$\begin{cases} \eta_1 + \xi_1 - BG_t Cos\theta_1 + T_{sf,1} + \dfrac{\dot{q}_{friction} A}{MD_{total} \dot{m} c_{p,fl}} = T_{inlet} \\ \left.\begin{aligned} &\eta_i e^{\lambda_1 L_i} + \xi_i e^{\lambda_2 L_i} + G_t L_i Cos\theta_i - BG_t Cos\theta_i + T_{sf,i} = \eta_{i+1} + \xi_{i+1} - BG_t Cos\theta_{i+1} + T_{sf,i+1} \\ &(1+\lambda_1 B)\eta_i e^{\lambda_1 L_i} + (1+\lambda_2 B)\xi_i e^{\lambda_2 L_i} + G_t L_i Cos\theta_i + T_{sf,i} = (1+\lambda_1 B)\eta_{i+1} + (1+\lambda_2 B)\xi_{i+1} + T_{sf,i+1} \end{aligned} \right\}_{i=1}^{n-1} \\ \eta_n \lambda_1 e^{\lambda_1 L_n} + \xi_n \lambda_2 e^{\lambda_2 L_n} + G_t Cos\theta_n = 0 \end{cases} \tag{25}$$

System (25) consists of $2n$ equations and $2n$ unknowns $\{\eta_i, \xi_i\}_{i=1}^{n}$. It can be solved by modified Gaussian elimination to acquire the final result for temperature profile of drillpipe and annular drilling fluid in each section.

The semi-analytical model has been employed and the results obtained were compared with those from Karstad [2]. With the same inputs, the two models generate a rather close match for temperature profiles (Appendix C – Figure 8).

3. EVALUATION OF FRICTIONAL HEAT SOURCE:

During drilling operations, frictional heat usually originates from the following two main sources: viscous friction and mechanical friction.

Viscous friction:

Viscous drag friction is created from contacts between tubing and formation/casing with the moving drilling fluid as a result of fluid viscosity effect. However, apart from the case of vertical wells, viscous friction is often of less significance when compared to mechanical friction in other circumstances. Therefore, heat generated from viscous drag is neglected in this study.

Mechanical friction:

– Friction at drillbit: A considerable amount of work has been done on this subject by various authors with different bit types. In this study, a general formula is used to estimate the heat generated at drillbit (originating from the work of Warren [5]):

$$\dot{q}_{bit} = \frac{1}{J}(1-\beta)\left(WOB * ROP + 2\pi N M_{bit}\right) \tag{26}$$

where:

J – Joule's constant (which relates the work done and heat generation, and is unity when both sides are in a consistent unit system),

β – bit efficiency (portion of work done by the drillbit that is used to break the rock),

WOB – weight on bit,

ROP – rate of penetration,

N – rotary speed (RPM),

M_{bit} – bit torque.

– Drag force between drillpipe and formation/casing:
In rotary drilling, heat generated from the drag force is one of the primary components. However, the effect of this factor on wellbore temperature profiles has not been addressed in recent studies. Therefore, in order to evaluate the value and significance of drag force, a 3D drag and torque model was investigated.
Details on the drag and torque model can be found from the work of Miska [4] and Mitchell [10] and is summarized in Appendix B. The unit contact force resulting from the drag and torque model, which subsequently relates to the drag force, is then utilized to estimate the heat generated by this mechanical drag:

- For rotary drilling:

$$\dot{q}_{drag} = \frac{1}{J} \int_{s_1}^{s_2} \mu \, w_c \, r_p \, 2\pi N \, ds \tag{27}$$

where:

J – Joule's constant,

μ – friction coefficient,

w_c – unit contact force,

r_p – outer radius of drillpipe,

N – rotary speed (RPM),

s – length, measured depth.

- For downhole motor drilling:

$$\dot{q}_{drag} = \frac{1}{J} \int_{s_1}^{s_2} \mu \, w_c \, ROP \, ds \tag{28}$$

where: ROP = rate of penetration.

The result obtained from the model was also compared with that from Landmark WellPlan software (Halliburton). Figure 9 in appendix C shows a good agreement between the 2 models.

4. MODEL ALGORITHM AND COMPUTER SIMULATOR:

A user friendly computer simulator was developed in Excel VBA (Visual Basic for Application). For flexibility and universality, the simulator also has a built-in unit conversion tool with units for both API and SI systems. The complete model is achieved by combining all individual components together using the algorithm shown in Appendix C – Figure 4.

Results & Discussion

The model is applied to a case study of a horizontal well. Complete inputs for the simulator can be found from Table 1 in Appendix C. The well trajectory is shown in Figure 3.

Figure 5 shows the transient effect of temperature profiles of drilling fluids under circulating condition (no drilling) at t = 2 h, 6 h and 10 h. As expected, this has an effect of cooling the wellbore fluid (bottomhole temperature is decreasing with time), since the inlet temperature is controlled at a constant value and it helps transfer the heat received from the formation out of the borehole.

In Figure 6, temperature profiles of drilling fluid in different operations are shown. It can be observed that bottomhole temperature reaches a very high value in rotary drilling mode (bottomhole temperature even exceeds formation temperature). On the other hand, in downhole motor drilling mode, the majority of additional heat added is due to the drillbit; the amount of frictional heat generated from drag force is negligible (3% of total mechanical heat sources) compared to rotary drilling (75% of total mechanical heat sources). This is because the rotary speed is much higher than the rate of penetration, and thus drag force in rotating mode is more significant than in sliding mode.

A sensitivity analysis of friction coefficient on drilling fluid temperature profile in rotary drilling is shown in Figure 7. The bottomhole temperature is under-predicted from 4% to 6% if mechanical friction is not taken into account. Another important point is that the drilling fluid return temperature seems to be similar for different cases while downhole temperature varies, indicating that misinterpretation of wellbore temperature may be taking place and could result in serious problems.

Besides the 2D case investigated above, the simulator is also capable of doing calculation for 3D cases. Figure 10 in appendix C shows an example of a 3D wellbore case. Taking inputs from wellbore surveys and other user-defined parameters, the program can generate temperature profiles for drilling fluid inside the drillpipe and annulus as a function of measured depth. A 3D wellbore trajectory with detail information is also included to provide visual enhancement and to quickly locate sections or points of interest.

CONCLUSIONS

1) In a horizontal well, bottomhole temperature in rotary drilling mode can exceed the virgin formation temperature.
2) Drilling fluid return temperature seems to have little difference in various operations, and thus may not be a good indication of downhole temperature conditions.

NOMENCLATURE

A – area
b – binormal
c_p – heat capacity
F – force
G_t – geothermal gradient
J – Joule's constant
k – thermal conductivity
L – length
MD – measured depth
M – torque, moment
m – mass flow rate
N – rotary speed
n – normal
q – heat rate
ROP – rate of penetration

r – radius
s – length, measured depth
T – temperature
t – time
U – overall heat transfer coefficient
WOB – weight on bit
z – depth

GREEK LETTERS

α – thermal diffusivity
β – bit efficiency
φ – contact force angle
κ – curvature
μ – friction coefficient
θ – inclination angle
τ – torsion

SUBSCRIPTS

a – annulus
c – contact
d – drillpipe
e – effective
f – formation
fl – fluid
sf – surface
t – tangential
w – wall
z – vertical

REFERENCES

[1] Dahl B., Saasen A.: *Heating of wells due to drilling operation.* Industry Presentation at The University of Tulsa Drilling Research – Advisory Board Meeting, 2006
[2] Karstad E.: *Analytical Approach to Temperature Induced Well Problems.* SPE To be published, 2009
[3] Hasan A.R., Kabir C.S.: *Fluid Flow and Heat Transfer in Wellbores.* Texas: Society of Petroleum Engineers, 2002, 670–674
[4] Aadnoy B., Cooper I., Miska S., Mitchell R., Payne M.: *Advanced Drilling and Well Technology*. SPE To be published in 2009
[5] Warren T.M.: *Factors Affecting Torque for a Roller Cone Bit.* Paper SPE 11994, 1984
[6] Holmes Charles S., Swift Samuel C.: *Calculation of Circulating Mud Temperatures.* Journal of Petroleum Technology, June, 1970, 670–674

[7] Hasan A.R., Kabir C.S., Ameen M.M., Kouba G.E.: *Determining Circulating Fluid Temperature in Drilling.* Workover, and Well-Control Operations," paper SPE 24581, 1996
[8] Raymond L.R.: *Temperature Distribution in a Circulating Drilling Fluid.* Journal of Petroleum Technology, March, 1969, 333–341
[9] Sawaryn S.J., Thorogood J.L.: *A Compendium of Directional Calculations Based on the Minimum Curvature Method.* Paper SPE 84246, 2005
[10] Mitchell Robert F., Samuel Robello: *How Good is the Torque-Drag Model?* Paper SPE/IADC 105068, 2007
[11] Chapman A. J.: *Heat Transfer*. New York: The Macmillan Company, 1967

APPENDICES

A – Dimensionless Time Model

– Hasan-Kabir (constant heat flux, cylindrical-source well):

$$f(t_D) = \left(1.1281\sqrt{t_D}\right)\left(1-0.3\sqrt{t_D}\right) \quad if\ 10^{-10} \le t_D \le 1.5$$
$$f(t_D) = \left(0.4063+0.5\ln t_D\right)\left(1+\frac{0.6}{t_D}\right) \quad if\ t_D > 1.5 \tag{A-1}$$

where:

$$t_D = \frac{\alpha_f t}{r_w^2}\times 3600 \tag{A-2}$$

– Chiu-Thakur (constant temperature at the wall, cylindrical source well):

$$f(t_D) = 0.982\ln\left(1+1.81t_D\right) \quad \text{for} \quad t_D \ge 0.1 \tag{A-3}$$

where:

$$t_D = \frac{\sqrt{\alpha_f t/24}}{r_w} \tag{A-4}$$

– Ramey (constant heat flow rate, line-source well):

$$f(t_D) = \ln\left(2\frac{\sqrt{\alpha_f t}}{r_w}\right) - 0.29 \tag{A-5}$$

B – 3D Soft String Drag and Torque Model – Ref 4

The simplified model applies the following assumptions:

- Pipe is in continuous contact with wellbore (no tool joints, couplings, wellbore irregularities or tortuosity effect);
- Inertia effect due to sliding and/or rotation are neglected;
- Fluid flow effects are not considered;
- Friction force is modeled using Coulomb friction concept;
- No consideration of buckling;
- Wellbore trajectory is modeled using minimum curvature method;
- The drillpipe has no bending rigidity and no shear forces.

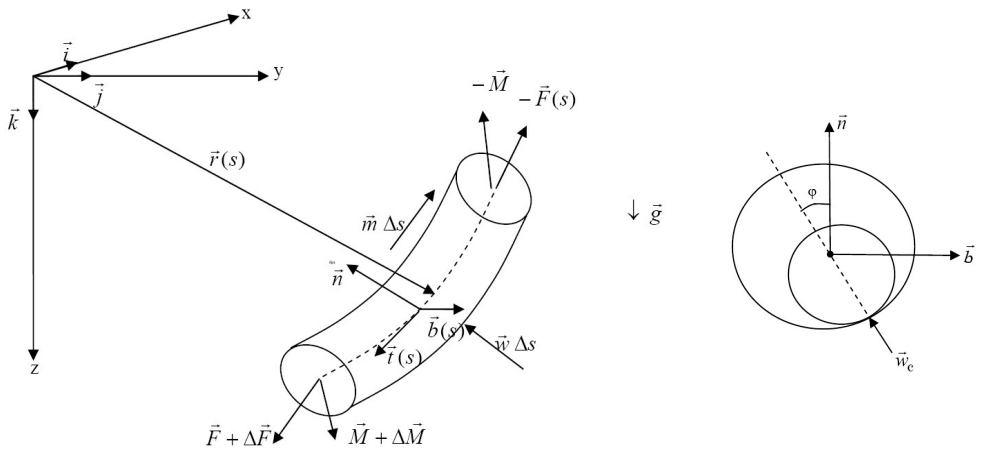

Fig. 1. Drag and torque analysis

A differential pipe element is considered in a right hand Cartesian coordinate system with unit vectors $\vec{i}, \vec{j}, \vec{k}$ as depicted in Figure 1. Furthermore, a Frenet – Serret local coordinate system is also introduced with unit vectors $\vec{t}, \vec{n}, \vec{b}$. The general formulation of force and moment equilibrium is developed as follows:

Equilibrium of force:

$$\frac{d\vec{F}}{ds} + \vec{w} = \vec{0} \tag{B-1}$$

where:

$$\begin{cases} \vec{F} = F_t\vec{t} + F_n\vec{n} + F_b\vec{b} \\ \vec{w} = \vec{w}_e + \vec{w}_c + \vec{w}_d \end{cases} \tag{B-2}$$

F_t – tangential (axial) force

F_n – shear force in normal direction

F_b – shear force in binormal direction

w_e – pipe effective unit weight

w_c – unit contact force

w_d – unit drag force

Equilibrium of moment:

$$\frac{d\vec{M}}{ds} + \vec{t} \times \vec{F} + \vec{m} = \vec{0} \tag{B-3}$$

where:

$$\begin{cases} \vec{M} = EI\,\kappa\vec{b} + M_t\vec{t} \\ \vec{m} = \vec{r}_p \times \vec{w}_d \end{cases} \tag{B-4}$$

EI – pipe bending stiffness

κ – pipe curvature

M_t – magnitude of moment required for pipe rotation

$\vec{r}_p$ – pipe radius vector

Combine equations (B-1) to (B-4), and obtain the corresponding scalar equations for force and moment equilibrium:

$$\begin{cases} \dfrac{dF_t}{ds} - \kappa F_n + w_e\vec{t} \bullet \vec{k} + \vec{w}_d \bullet \vec{t} = 0 \\ \dfrac{dF_n}{ds} + \kappa F_t - F_b\tau + w_e\vec{n} \bullet \vec{k} + \vec{w}_d \bullet \vec{n} + \vec{w}_c \bullet \vec{n} = 0 \\ \dfrac{dF_b}{ds} + F_n\tau + w_e\vec{b} \bullet \vec{k} + \vec{w}_d \bullet \vec{b} + \vec{w}_c \bullet \vec{b} = 0 \end{cases} \tag{B-5}$$

$$\begin{cases} \dfrac{dM_t}{ds} + \vec{m} \bullet \vec{t} = 0 \\ \kappa M_t - EI\,\kappa\tau - F_b + \vec{m} \bullet \vec{n} = 0 \\ EI\,\dfrac{d\kappa}{ds} + F_n + \vec{m} \bullet \vec{b} = 0 \end{cases}$$

System (B-5) consists of 6 scalar equations that can be solved simultaneously for the desired components of forces and moments along the string.

– In sliding mode, $M_t = 0$ along the string. Apply simplifying assumptions, (B-5) reduces to:

$$\begin{cases} \dfrac{dF_t}{ds} + w_e t_z \pm \mu w_c = 0 \\ F_t \kappa + w_e n_z + w_c \cos\varphi = 0 \\ w_e b_z - w_c \sin\varphi = 0 \end{cases} \tag{B-6}$$

where φ is the contact force angle as shown in Figure 1.
The unit contact force can be calculated as follows:

$$\begin{cases} w_c = \sqrt{\left(F_t \kappa + w_e n_z\right)^2 + \left(w_e b_z\right)^2} \\ \dfrac{dF_t}{ds} + w_e t_z \pm \mu w_c = 0 \end{cases} \tag{B-7}$$

– In rotating mode, (B-5) reduces to:

$$\begin{cases} \dfrac{dF_t}{ds} + w_e t_z = 0 \\ \kappa F_t + w_e n_z + w_c \cos\varphi + \mu w_c \sin\varphi = 0 \\ w_e b_z - w_c \sin\varphi + \mu w_c \cos\varphi = 0 \end{cases} \tag{B-8}$$

$$\begin{cases} \dfrac{dM_t}{ds} - \mu w_c r_p = 0 \\ M_t \kappa = 0 \end{cases}$$

It is observed that the weakness of this simplified model is that the last equation in (B-8) cannot be satisfied.
The unit contact force is calculated from:

$$\begin{cases} \dfrac{dF_t}{ds} + w_e t_z = 0 \\ w_c = \sqrt{\dfrac{\left(F_t \kappa + w_e b_z\right)^2 + \left(w_e b_z\right)^2}{1 + \mu^2}} \end{cases} \tag{B-9}$$

C – Figures and Graphs

Table 1
Inputs for case study

Drillpipe ID	3.958	in
Drillpipe OD	4.5	in
Hole Diameter	8.5	in
Pipe Unit Weight in Air	12.75	lb/ft
Pipe Thermal Conductivity	20	BTU/(h.ft.°F)
Fluid Density	10	ppg
Fluid Specific Heat Capacity	0.4	BTU/(lb.°F)
Fluid Thermal Conductivity	1	BTU/(h.ft.°F)
Fluid Viscosity	110	lb/(ft.h)
Fluid Inlet Temperature	75	°F
Formation Density	165	lb/ft3
Formation Specific Heat Capacity	0.2	BTU/(lb.°F)
Formation Thermal Conductivity	1.3	BTU/(h.ft.°F)
Formation Surface Temperature	60	°F
Geothermal Gradient	0.0127	°F/ft
Circulation Rate	300	gpm
ROP	50	ft/h
Rotary speed	100	RPM
Time	10	h
WOB	5	kip
Bit Torque	1000	ft.lbf
Friction Coefficient	0.3	
Bit Efficiency	80%	

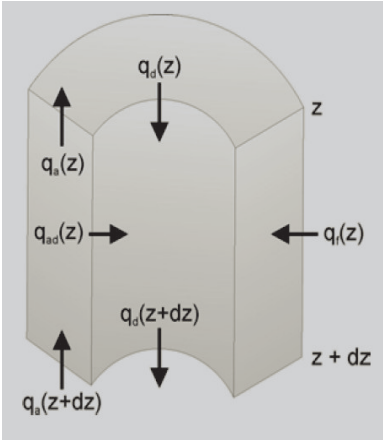

Fig. 2. Heat rates in the control volume

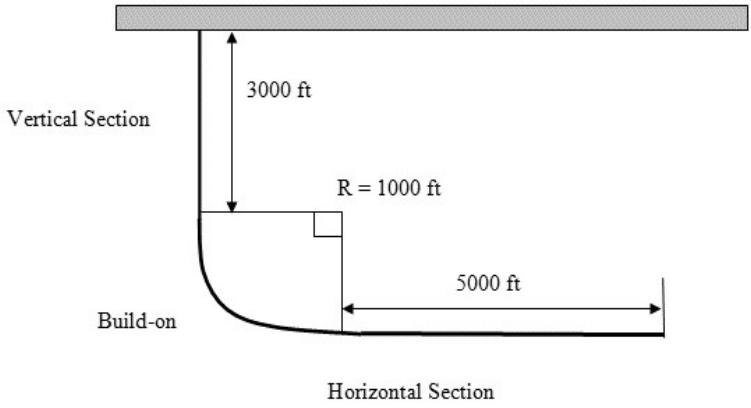

Fig. 3. Well trajectory for case study

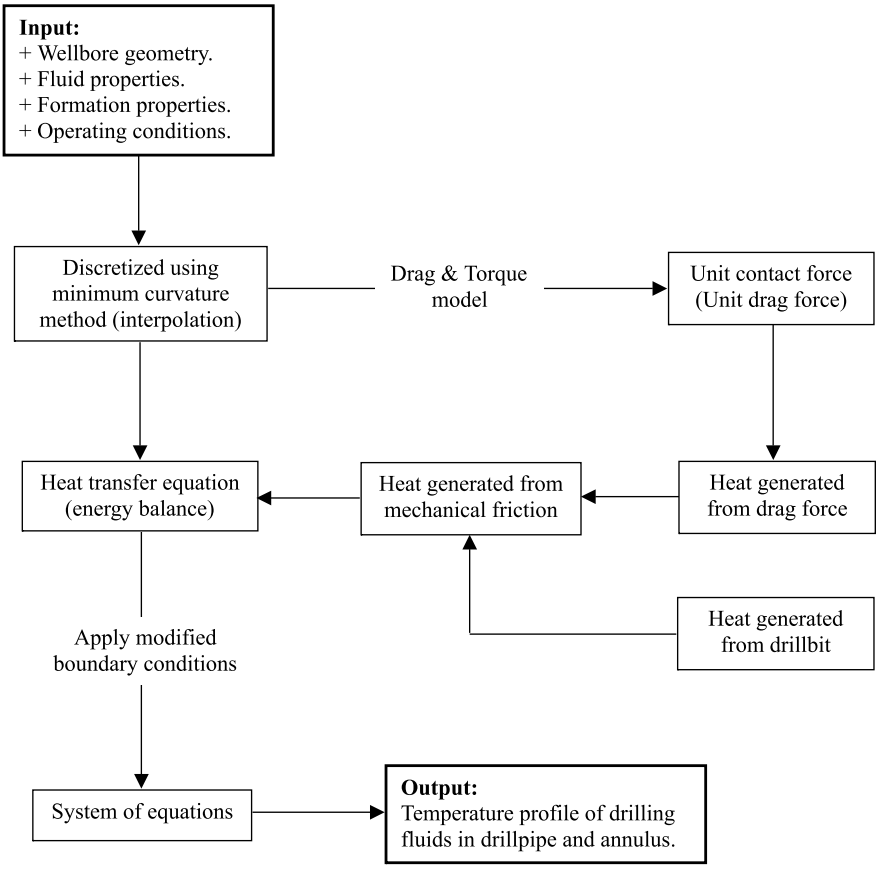

Fig. 4. Model algorithm

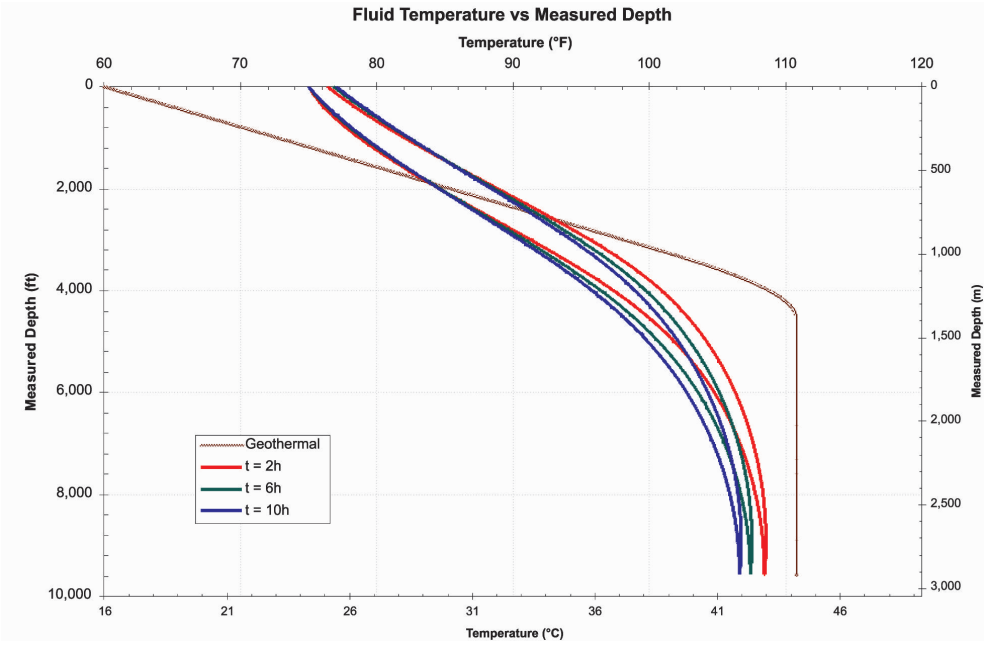

Fig. 5. Circulating fluid temperature profiles at different time, *t*

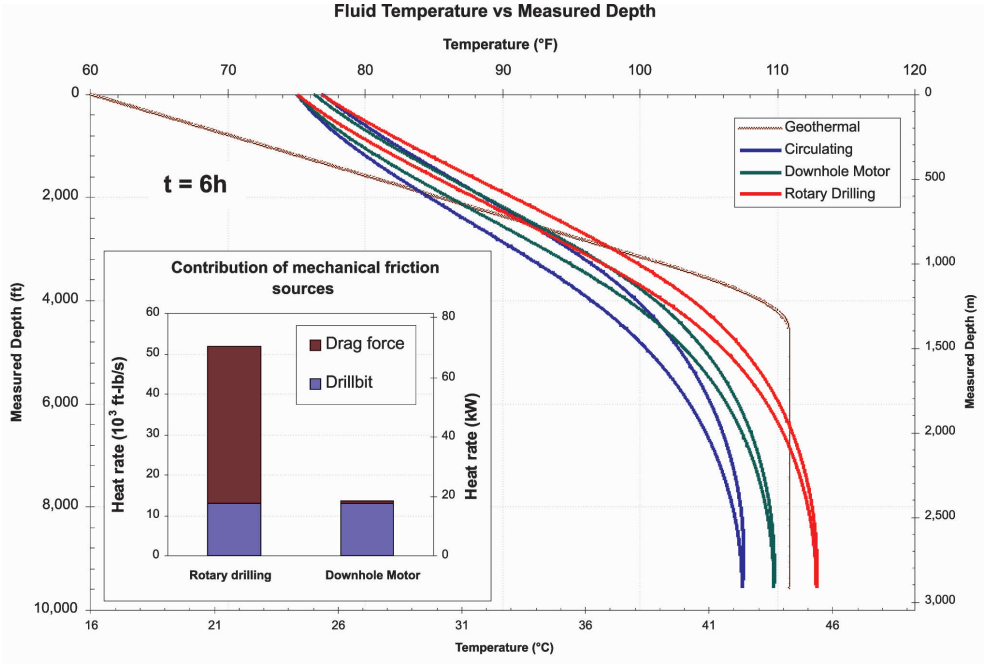

Fig. 6. Fluid temperature profiles at different operating conditions

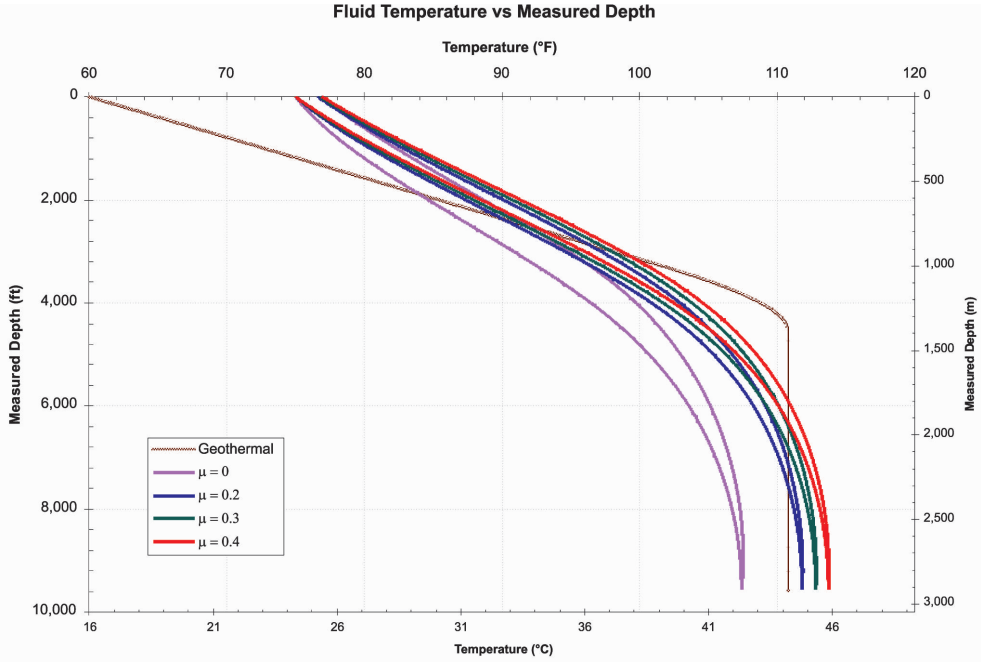

Fig. 7. Fluid temperature profiles at different friction coefficients in rotary drilling mode

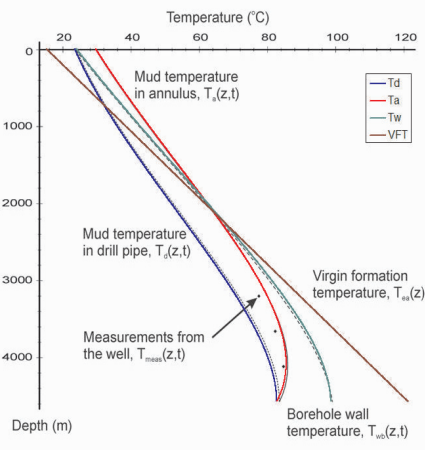

Fig. 8. Compare temperature profiles obtained from model with those from Karstad

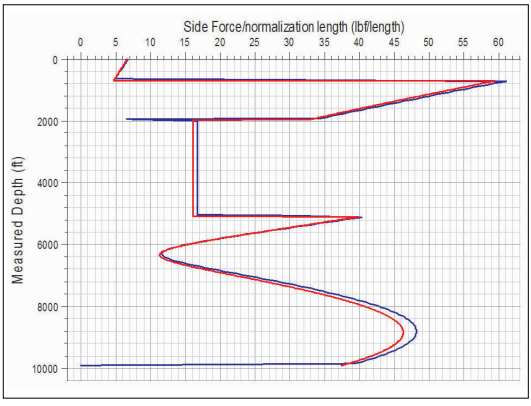

Fig. 9. Compare unit contact force obtained from model with that from Landmark WellPlan (Halliburton)

MD (ft)	Inclination Angle (deg)	Azimuth
0	3.75	N45E
702.5	5.5	N45E
1964.5	29.75	N77E
4250	29.75	N77E
5086.3	29.75	N77E
8504.1	80.89	N59.3W
8828	90	N62.7W
9151.9	99.11	N66.1W
9901.7	120	N75W

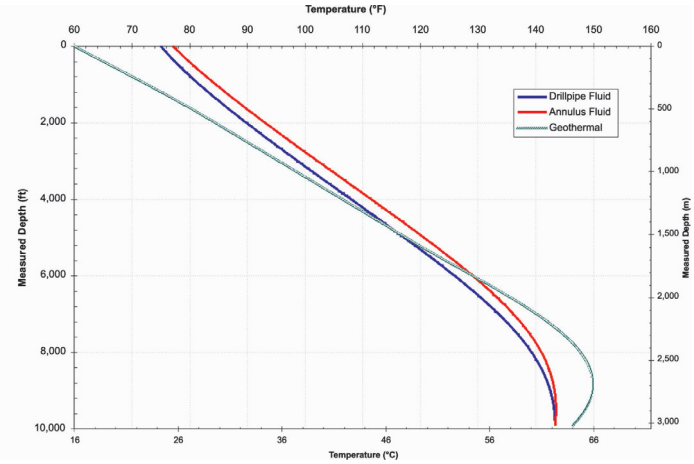

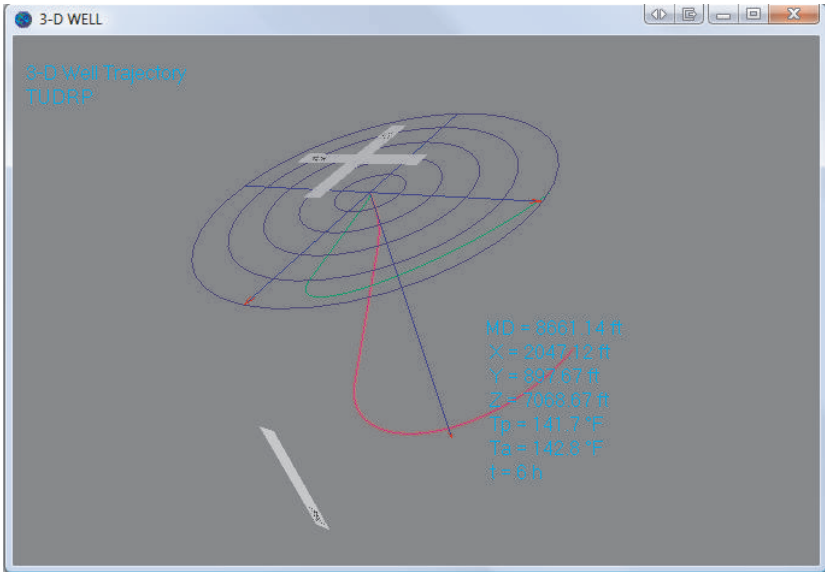

Fig. 10. Calculation for a 3D case